



OPEN

SUBJECT AREAS:

BREEDING
RUBISCOAGRICULTURAL GENETICS
QUANTITATIVE TRAITReceived
4 March 2013Accepted
18 June 2013Published
29 August 2013Correspondence and
requests for materials
should be addressed to
T.Y. (toshiyama@affrc.
go.jp)* These authors
contributed equally to
this work.

A natural variant of *NAL1*, selected in high-yield rice breeding programs, pleiotropically increases photosynthesis rate

Toshiyuki Takai^{1,3*}, Shunsuke Adachi^{2,3*}, Fumio Taguchi-Shiobara³, Yumiko Sanoh-Arai¹, Norio Iwasawa¹, Satoshi Yoshinaga¹, Sakiko Hirose¹, Yojiro Taniguchi¹, Utako Yamanouchi³, Jianzhong Wu³, Takashi Matsumoto³, Kazuhiko Sugimoto³, Katsuhiko Kondo³, Takashi Ikka³, Tsuyu Ando⁴, Izumi Kono⁴, Sachie Ito⁴, Ayahiko Shomura⁴, Taiichiro Ookawa², Tadashi Hirasawa², Masahiro Yano³, Motohiko Kondo¹ & Toshio Yamamoto³

¹NARO Institute of Crop Science, Tsukuba, Ibaraki 305-8508, Japan, ²Graduate School of Agriculture, Tokyo University of Agriculture and Technology, Fuchu, Tokyo 183-8509, Japan, ³National Institute of Agrobiological Sciences, Tsukuba, Ibaraki 305-8602, Japan, ⁴Institute of the Society for Techno-innovation of Agriculture, Forestry and Fisheries, Tsukuba, Ibaraki 305-0854, Japan.

Improvement of leaf photosynthesis is an important strategy for greater crop productivity. Here we show that the quantitative trait locus *GPS* (*GREEN FOR PHOTOSYNTHESIS*) in rice (*Oryza sativa* L.) controls photosynthesis rate by regulating carboxylation efficiency. Map-based cloning revealed that *GPS* is identical to *NAL1* (*NARROW LEAF1*), a gene previously reported to control lateral leaf growth. The high-photosynthesis allele of *GPS* was found to be a partial loss-of-function allele of *NAL1*. This allele increased mesophyll cell number between vascular bundles, which led to thickened leaves, and it pleiotropically enhanced photosynthesis rate without the detrimental side effects observed in previously identified *nali* mutants, such as dwarf plant stature. Furthermore, pedigree analysis suggested that rice breeders have repeatedly selected the high-photosynthesis allele in high-yield breeding programs. The identification and utilization of *NAL1* (*GPS*) can enhance future high-yield breeding and provides a new strategy for increasing rice productivity.

Rice (*Oryza sativa* L.) is a staple food that feeds nearly half of the world's population. Over the past half century, rice production has more than doubled owing to the advent of high-yielding semi-dwarf cultivars, including IR8, sometimes called "miracle rice". IR8 has a short-stature phenotype, caused by the *sd1* (*semi-dwarf1*) gene, which enables the plant to resist lodging and thus allows treatment with higher levels of fertilizer, resulting in high yields. This surprising success contributed to the "Green Revolution"^{1,2}. However, the current world population of over 7 billion and the predicted growth to 9 billion by 2050 will require a 60% to 70% further increase in rice production without a corresponding increase in the amount of agricultural land^{3,4}.

Rice yield is determined by the balance of a number of factors, including sink size, source strength, and carbohydrate translocation. Several genes underlying quantitative trait loci (QTLs) associated with sink size have been identified, including several for grain number regulation (*GN1a*⁵, *APO1*⁶, and *WFP*⁷) and grain size regulation (*GW2*⁸, *GS3*⁹, *qSW5*¹⁰, and *GS5*¹¹). However, near-isogenic lines (NILs) having favourable *GN1a* and *APO1* alleles have not markedly improved yield in the *japonica* genetic background, illustrating the importance of the balance among sink size, source strength, and carbohydrate translocation for attaining high yield¹².

Leaf photosynthesis is one of the main aspects of source strength, and rice simulation models indicate that leaf photosynthesis, particularly in flag leaves, plays an important role in determining crop yield^{13,14}. Wide natural variation in light-saturated photosynthesis rate under ambient CO₂ concentration has been observed among rice cultivars^{15,16}. The photosynthesis rate is generally determined by both CO₂ supply to chloroplasts and demand for CO₂ in the chloroplasts^{17,18}. The CO₂ supply is governed by diffusion of CO₂ from the atmosphere through stomata to the sites of carboxylation in the chloroplasts. One of the factors involved in the CO₂ supply is stomatal



conductance, an indication of stomatal aperture¹⁷. The demand for CO₂ is governed by the rate of CO₂ processing in the chloroplast. One of the factors involved in the demand for CO₂ is the amount of active ribulose 1,5-bisphosphate carboxylase/oxygenase (Rubisco)¹⁸. Because large amounts of nitrogen (N) are invested in Rubisco, leaf N content is also recognized as an important factor for photosynthesis^{19,20}. The natural variation in photosynthesis rate is well explained by variation in both stomatal conductance and leaf N content^{21,22}. While these eco-physiological characteristics of rice photosynthesis have been elucidated, genes associated with the variation in photosynthesis rate are yet to be identified, owing to the complexity of this trait^{23,24}.

In this study, QTL analysis combined with map-based cloning using Takanari, a high-yielding, high-photosynthesis rice cultivar, led to the identification and isolation of a major QTL controlling the photosynthesis rate in flag leaves of rice. An NIL carrying the favourable allele for this QTL had an enhanced photosynthesis rate caused by an increase in carboxylation efficiency, which originated from pleiotropic effects of leaf anatomical modifications. A subsequent pedigree analysis revealed that rice breeders have repeatedly selected this allele in high-yield breeding programs. These results suggest that the identification and utilization of photosynthesis-related QTLs can enhance future high-yield breeding and provide a new strategy for achieving increased rice productivity.

Results

QTL analysis. To identify genes controlling photosynthesis rate, we chose a high-yielding *indica* rice cultivar, Takanari, and a leading *japonica* cultivar, Koshihikari, both grown in Japan. Takanari has

one of the highest photosynthesis rates among cultivars in global rice core collections²¹, and the greatest difference in photosynthesis rate between Koshihikari and Takanari at any time during the growth period was in flag leaves at the full heading stage²⁵. Takanari, which is descended from high-yielding cultivars including IR8 (Fig. 1a), possesses the *sd1* gene²⁶ and has shorter plant stature but darker green and wider flag leaves than Koshihikari (Fig. 1b, c). As expected, the photosynthesis rate of flag leaves at the full heading stage was higher in Takanari than in Koshihikari (Fig. 1d). Leaf N content and stomatal conductance were also higher in Takanari than in Koshihikari (Fig. 1e, f).

We developed primary mapping populations of reciprocal back-cross inbred lines (BILs) derived from a cross between Koshihikari and Takanari. Both sets of BILs, consisting of 82 lines in the Koshihikari genetic background and 86 in the Takanari background, were used to make detection and mapping of QTLs more precise. We measured the leaf photosynthesis rate in flag leaves of the reciprocal BILs at the full heading stage with a portable photosynthesis system (LI-6400; Li-Cor) under an optimal and constant leaf chamber conditions in the morning on clear days. Photosynthesis rate showed continuous variation in both mapping populations (Supplementary Fig. S1). QTL analysis with 140 molecular markers detected two QTLs in the Koshihikari background and four in the Takanari background (Supplementary Fig. S1, Supplementary Table S1). Among them, a QTL on the long arm of chromosome 4 was commonly detected in both mapping populations, with the allele from Takanari contributing to an increase in photosynthesis rate. Our earlier studies also found QTLs associated with photosynthesis-related traits such as chlorophyll content on the long arm of

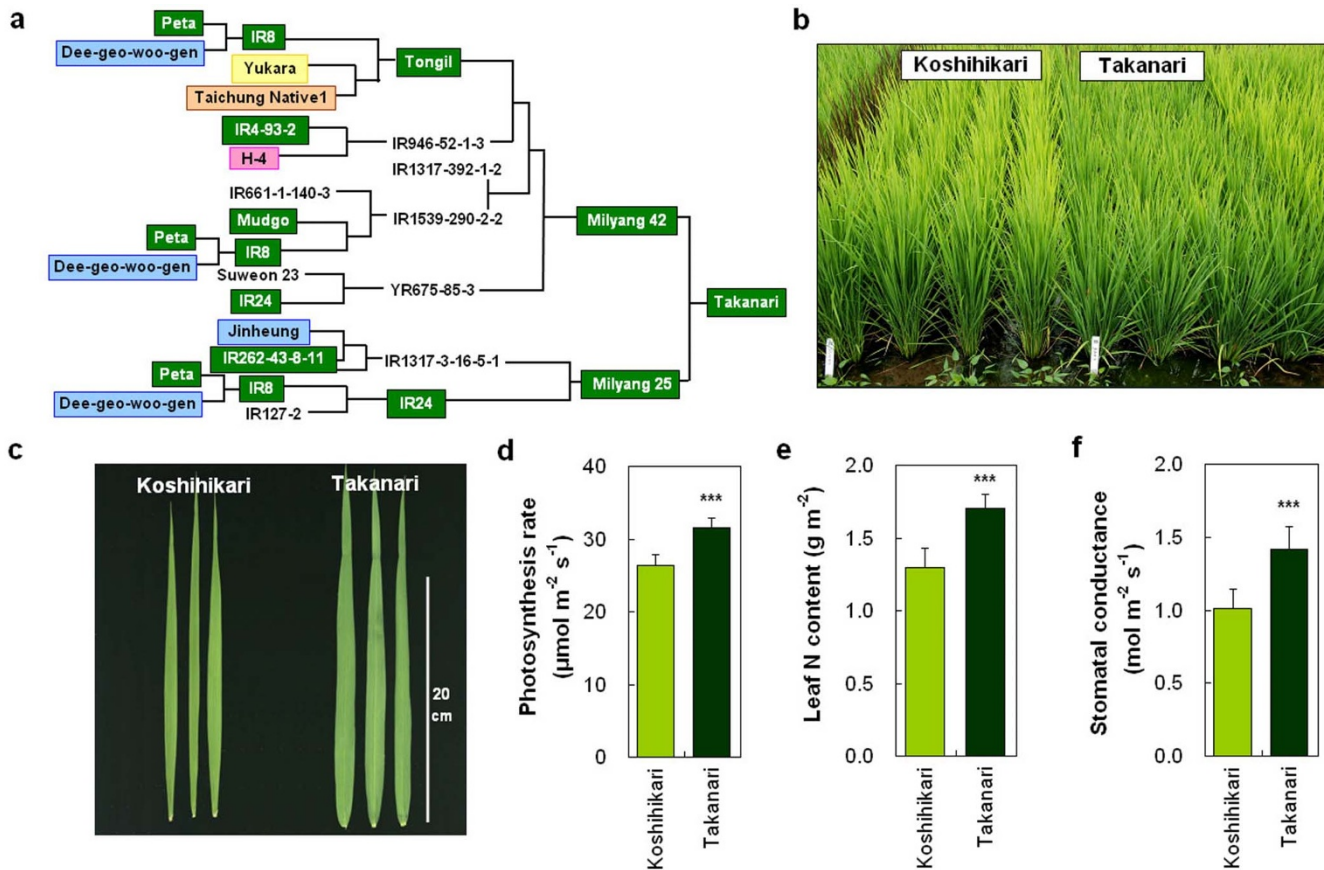


Figure 1 | Characteristics of high-yielding rice cultivar Takanari. (a) Pedigree of Takanari. Cultivars marked with the same colour box have the same GPS haplotype. (b, c) Plant morphology (b) and flag leaves (c) of field-grown Koshihikari and Takanari. (d–f) Comparisons of photosynthesis rate (d), N content (e), and stomatal conductance (f) of flag leaves at full heading stage between Koshihikari and Takanari. Each column represents mean \pm s.d. ($n = 18$); *** $P < 0.001$ versus Koshihikari (Student's *t*-test).



chromosome 4^{27,28}. Thus, we selected this QTL, here named *GREEN FOR PHOTOSYNTHESIS* (*GPS*), for further analysis.

Physiological characterization of *GPS*. For map-based cloning and characterization of QTLs, we developed reciprocal NILs-*GPS*, each carrying the *GPS* region from either Koshihikari or Takanari in the genetic background of the other (Fig. 2a). Koshihikari NIL-*GPS* (i.e., Koshihikari background containing *GPS* from Takanari) had darker

green leaves than Koshihikari, and Takanari NIL-*GPS* had lighter green leaves than Takanari (Fig. 2a). Comparison of flag leaf photosynthesis rates confirmed the effect of *GPS*: Koshihikari NIL-*GPS* had a higher photosynthesis rate per unit leaf area than Koshihikari, and Takanari NIL-*GPS* had a lower photosynthesis rate than Takanari (Fig. 2b). These differences in photosynthesis rate were observed even when expressed per unit dry weight (Fig. 2c). Higher photosynthesis rates were associated with

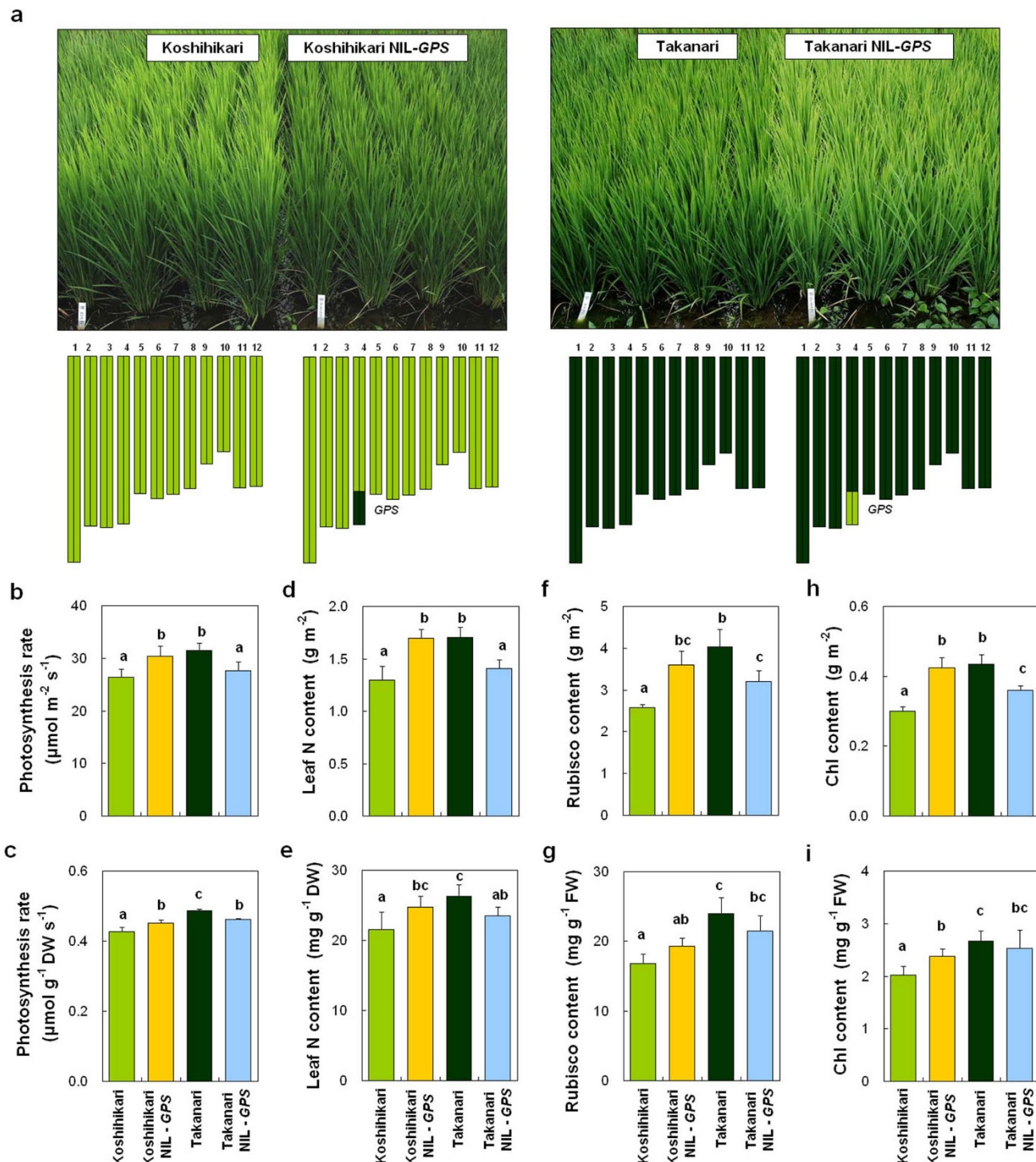


Figure 2 | Physiological characterization of *GPS* alleles. (a) Plant morphology and graphical genotypes of Koshihikari, Koshihikari NIL-*GPS*, Takanari, and Takanari NIL-*GPS*. Yellow-green bars, chromosome regions from Koshihikari; dark green, Takanari. (b–i) Comparisons of photosynthesis rate (b, c), leaf N content (d, e), Rubisco content (f, g), and chlorophyll (Chl) content (h, i) of flag leaves at full heading stage. Each column represents mean \pm s.d. ($n = 9$). Different letters indicate significant difference at the 5% level (Tukey–Kramer HSD test).



enhanced leaf N, Rubisco, and chlorophyll contents per unit leaf area, and in some cases per unit fresh or dry weight (Fig. 2d–i). Koshihikari NIL-GPS also exhibited greater responses to light and CO₂ than did Koshihikari, most notably a higher initial slope of the CO₂ response curve, reflecting higher carboxylation efficiency (Fig. 3a, b). According to a biochemical model of C₃ photosynthesis (the “Farquhar model”), photosynthesis rate is limited either by ribulose-1,5-bisphosphate (RuBP) carboxylation by Rubisco (carboxylation efficiency) or by RuBP regeneration in response to CO₂ concentration²⁹. To examine which step limited the photosynthesis rate in the parental cultivars and the reciprocal NILs-GPS under our experimental conditions (light saturation and ambient CO₂), we fitted the model to the CO₂ response data. Analysis revealed that the photosynthesis rate in all cultivars and NILs-GPS was limited by RuBP carboxylation by Rubisco (Supplementary Fig. S2). These results indicate that the primary role of GPS is related to carboxylation efficiency during photosynthesis. We further examined the relationship between Rubisco content and V_{c,max}, the maximum rate of RuBP carboxylation by Rubisco, obtained from the model-fitting analysis. V_{c,max} was closely related to Rubisco content (Supplementary Fig. S3). These results suggest that the increase in Rubisco content seen in lines containing the Takanari allele of GPS led to an increase in V_{c,max}, in turn increasing carboxylation efficiency and consequently photosynthesis rate. On the other hand, no significant difference was observed in stomatal conductance between each parental cultivar and the corresponding NIL-GPS (Supplementary Fig. S4). Neither stomatal density nor stomatal length differed between each parental cultivar and the corresponding NIL-GPS (Supplementary Fig. S4).

Cloning of GPS. For map-based cloning of GPS, we first used 142 F₂ plants derived from Koshihikari × Koshihikari NIL-GPS and 143 from Takanari × Takanari NIL-GPS. GPS was coarsely mapped near the simple sequence repeat (SSR) molecular marker RM3534 in both populations (Fig. 4a, b). For further high-resolution mapping, another 8308 and 2784 F₂ plants were used to select plants with recombination near RM3534 through marker-assisted selection in the Koshihikari and Takanari genetic backgrounds, respectively. From this selection, we obtained 26 and 24 plants, respectively. Analysis of recombinant homozygous F₃ lines narrowed the candidate region down to the 23.5-kb region between the markers InDel_4_135 and InDel_4_105 in both genetic backgrounds (Fig. 4a, b). The photosynthesis rates in lines carrying the Takanari allele in this region were higher than in those carrying the Koshihikari allele (Fig. 4a, b). The Rice Annotation Project Database (RAP-DB)³⁰

predicts three genes in this region. A bacterial artificial chromosome (BAC) clone containing the candidate genomic region (Taka03G22; Fig. 4b) was obtained by screening a genomic library of Takanari. We determined the sequence of the candidate region in Takanari by using this BAC clone and compared it with the corresponding sequence in Koshihikari, for which the whole genome sequence is now available³¹. Among the three genes annotated in RAP-DB, we found polymorphisms in the coding region for only one gene, at Os04g0615000. This gene was previously reported as NARROW LEAF1 (*NAL1*), encoding a plant-specific protein which may be involved in polar auxin transport³². There were ten single-nucleotide polymorphisms (SNPs), three of which encoded amino acid substitutions, in *NAL1* between Koshihikari and Takanari (Fig. 4c). A 5895-bp retrotransposon insertion was also found in the second exon of *NAL1* in the Koshihikari genome (Fig. 4c).

The previously identified *nall* mutation affected plant height as well as lateral leaf growth³². However, the relationship between *NAL1* and leaf photosynthesis was not examined in that study. To clarify the effect of *NAL1* on leaf photosynthesis, we analysed a *nall* mutant in the Taichung 65 genetic background (T65-*nall*), which has the same deletion of 30-bp in the fourth exon as previously reported³² (Fig. 4c). T65-*nall* showed severe dwarf plant stature and remarkably smaller and narrower flag leaves than T65 (Fig. 5a, b, Supplementary Fig. S5a–c). However, T65-*nall* had higher flag leaf N content both per unit leaf area and per unit dry weight at full heading than T65 (Fig. 5c, d) and a higher photosynthesis rate than T65 (Fig. 5e). These results suggest that reduction or loss-of-function of *NAL1* increased photosynthesis rate.

To confirm that *NAL1* controls photosynthesis rate, we generated RNA interference (RNAi) transgenic plants to decrease the expression level of *NAL1* in the Koshihikari genetic background (RNAi-*NAL1*). The RNAi-*NAL1* plants (T₀) showed dwarf plant stature and smaller and narrower flag leaves than Koshihikari (Fig. 5f, Supplementary Fig. S5e–g), and the reduced levels of *NAL1* expression induced a higher photosynthesis rate in the flag leaves of the RNAi-*NAL1* plants at full heading (Fig. 5g). The enhanced photosynthesis rate was associated with higher flag leaf N content (Fig. 5h, i). Thus, we conclude that *NAL1* pleiotropically controls both plant stature and photosynthesis rate and corresponds to GPS.

When we compared the flag leaf shapes and culm lengths of Koshihikari, Takanari, the reciprocal NILs-GPS, T65-*nall*, and RNAi-*NAL1*, flag leaf width and length in Koshihikari NIL-GPS were decreased compared with Koshihikari (Fig. 6a, Supplementary Fig. S5i, j), but the reduction was less severe than in T65-*nall* and RNAi-*NAL1* (Supplementary Fig. S5a, b, e, f, i, j). No difference was

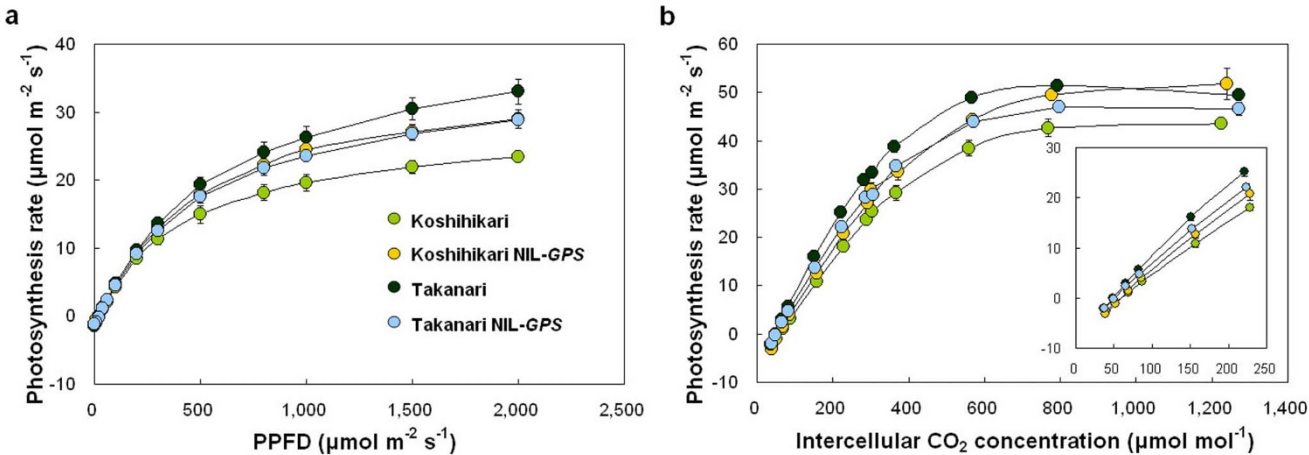


Figure 3 | Responses of GPS to light and CO₂. (a) Effect of light intensity on photosynthesis in flag leaves at full heading stage in Koshihikari, Koshihikari NIL-GPS, Takanari, and Takanari NIL-GPS (n = 3). PPFD, photosynthetic photon flux density. (b) Effect of intercellular CO₂ concentration on photosynthesis in flag leaves at full heading stage in the four genotypes (n = 3).

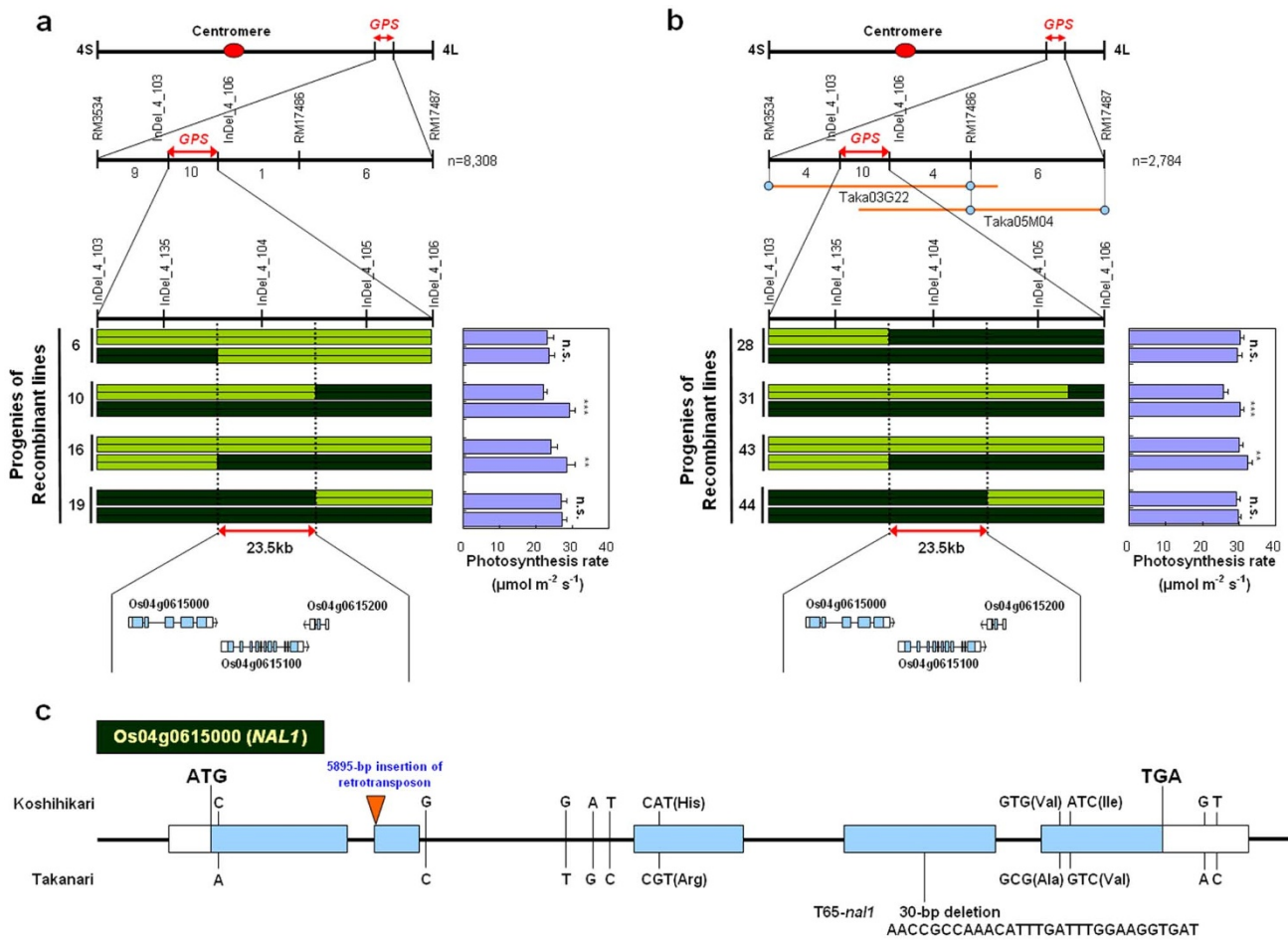


Figure 4 | Molecular cloning of GPS. (a, b) High-resolution linkage map of GPS region produced with 8308 F₂ plants in the Koshihikari background (a) and 2784 F₂ plants in the Takanari background (b). Populations were produced by crossing each cultivar with the corresponding NIL-GPS. The number of recombinants between molecular markers is indicated below the second line in each figure part. Yellow-green shading, regions homozygous for alleles from Koshihikari; dark green, Takanari. Each purple bar in the photosynthesis rate graphs represents the mean \pm s.d. (n = 6) of the adjacent genotype. ***P < 0.001, **P < 0.01; n.s., not significant within pairs of recombinant lines (Student's t-test). (c) Gene structure and mutation sites of *NAL1* in Koshihikari, Takanari, and *nal1* mutant line in Taichung 65 genetic background (T65-*nal1*). Light blue bars represent exons; white bars represent 5' and 3' untranslated regions.

observed in culm length between each parental cultivar and the corresponding NIL-GPS (Supplementary Fig. S5k). On the basis of these results, we considered that the Takanari GPS allele might be functional but weaker than the Koshihikari allele. On the other hand, the presence of a retrotransposon insertion in the coding region of Koshihikari (Fig. 4c) might reduce the function relative to the Takanari allele. Therefore, we compared the expression level of *NAL1* in the flag leaves of Koshihikari and Takanari at several developmental stages. Quantitative real-time PCR (qRT-PCR) detected the expression of *NAL1* in both Koshihikari and Takanari, with no significant difference at any flag leaf developmental stage (Fig. 6b). Further investigation of *NAL1* transcripts found that about 20% of the Koshihikari transcripts sequenced contained no retrotransposon insertion, whereas many other transcripts sequenced contained insertion of the full, or partial retrotransposon (Supplementary Fig. S6). Takanari also had many splice variants in *NAL1* transcripts (Supplementary Fig. S7). Although a recent study reported several kinds of splice variants for *NAL1* transcripts only in an *indica* cultivar³³, our results revealed many splice variants for *NAL1* transcripts in both a *japonica* cultivar, Koshihikari, and an *indica* cultivar, Takanari. These results indicate that *NAL1* expression mechanism is too complicated to explain the cause of the two alleles of GPS by the expression or transcription level of *NAL1*.

Then, we next examined the level of NAL1 protein in the flag leaves of Koshihikari and Takanari. Western blot analysis detected a 64-kDa protein band corresponding to NAL1 in both Koshihikari and Takanari, but the signal was less abundant in Takanari (Fig. 6c). These results suggest that the three amino acid substitutions or the different levels of NAL1 protein might have been the cause of the difference in *NAL1* function in the two cultivars, detected in this study as the two alleles of GPS, although the detailed mechanisms underlying the differences between these alleles are still unknown.

Mechanisms underlying control of photosynthesis rate by *NAL1*. The finding that GPS and *NAL1* are the same gene suggests that leaf morphological changes affect the photosynthesis rate. Previous studies have shown that leaf anatomical changes can affect leaf photosynthesis^{34,35}. We examined specific leaf area (SLA), which is inversely related to leaf thickness³⁶, of flag leaves in Koshihikari, Takanari, and the reciprocal NILs-GPS, and found that the Takanari allele of GPS decreased SLA (Fig. 7a). Both T65-*nal1* mutant plants and RNAi-*NAL1* transgenic plants also showed lower SLA than either wild-type cultivar (Supplementary Fig. S5d, h). We next observed cross-sections of the central parts of flag leaves in Koshihikari, Takanari, and the reciprocal NILs-GPS, and confirmed that the Takanari allele increased leaf thickness at both

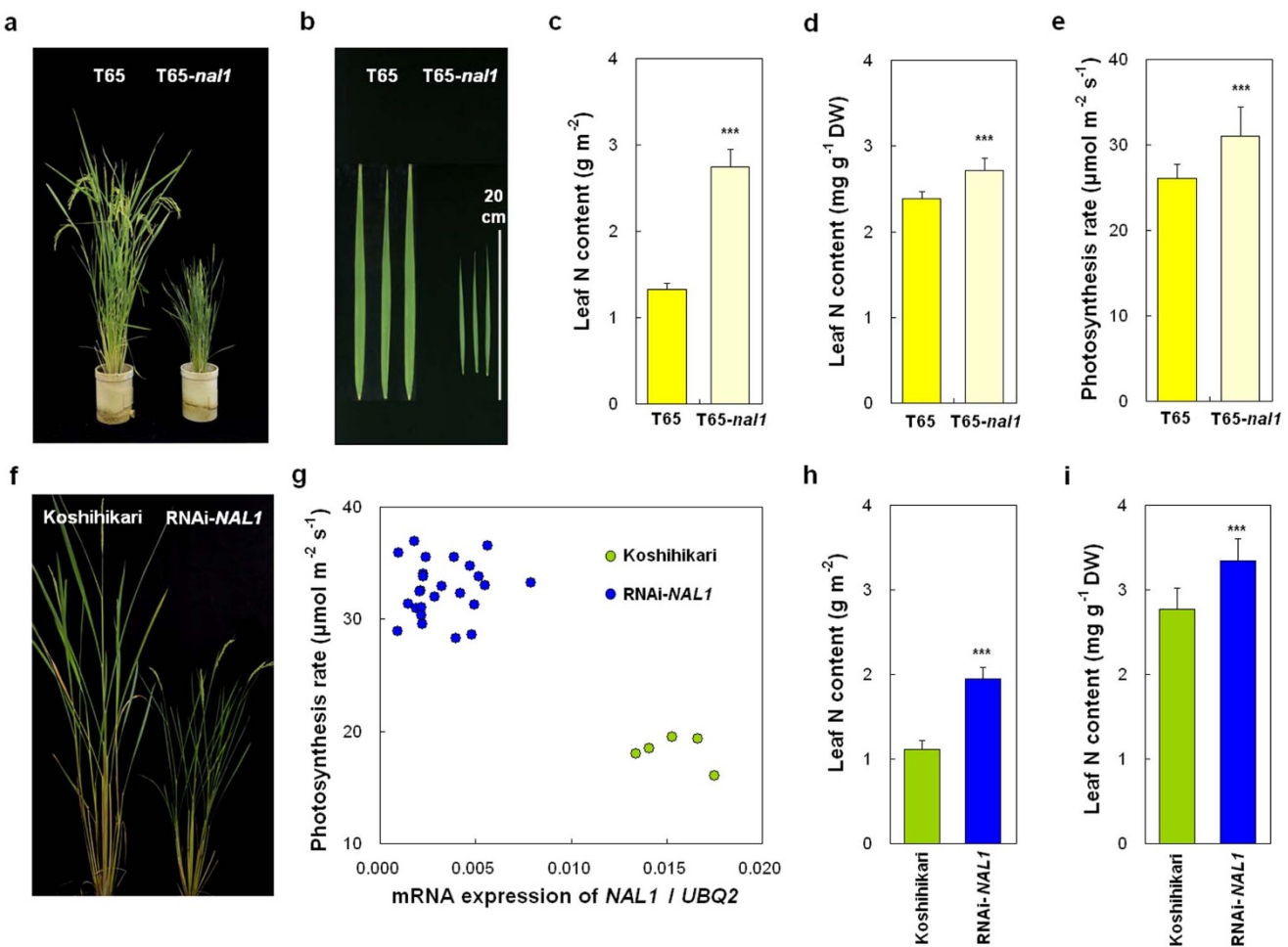


Figure 5 | Plant morphology and photosynthesis rate in mutant and transgenic plants with differing expression of *NAL1*. (a, b) Plant morphology (a) and flag leaves (b) of Taichung 65 (T65) and *nal1* mutant line in T65 genetic background (T65-nal1). (c–e) Comparison of N content per unit leaf area (c), N content per unit dry mass (d), and photosynthesis rate (e) of flag leaves at full heading stage between T65 and T65-nal1. Each column represents mean \pm s.d. ($n = 10$); *** $P < 0.001$ versus T65 (Student's *t*-test). (f) Plant morphology of Koshihikari and transgenic plants with RNAi-induced suppression of *NAL1* in the Koshihikari genetic background (RNAi-NAL1). (g) Relationship between expression level of *NAL1* and photosynthesis rate of flag leaves at full heading stage in Koshihikari and RNAi-NAL1 T₀ plants. Each circle represents an individual Koshihikari or T₀ plant. (h, i) Comparison of N content per unit leaf area (h) and per unit dry mass (i) between Koshihikari and RNAi-NAL1. Each column represents mean \pm s.d. ($n = 25$ for RNAi-NAL1, $n = 5$ for Koshihikari); *** $P < 0.001$ versus Koshihikari (Student's *t*-test).

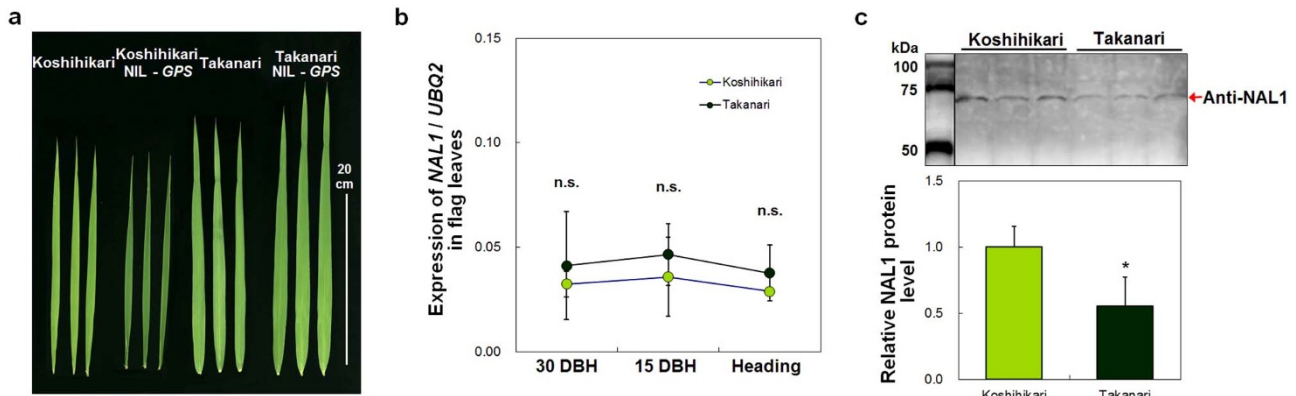


Figure 6 | Expression and protein differences between GPS alleles in Koshihikari and Takanari. (a) Flag leaves in Koshihikari, Koshihikari NIL-GPS, Takanari, and Takanari NIL-GPS. (b) Expression analysis by quantitative real-time PCR of *NAL1* in flag leaves at three developmental stages. DBH, days before heading. Each symbol represents mean \pm s.d. ($n = 4$); n.s., not significant between Koshihikari and Takanari (Student's *t*-test). (c) Western blot analysis of *NAL1* protein extracted from flag leaves. Molecular weight marker and samples were run on the same gel and were electrotransferred onto the same membranes. Each column in the graph represents mean \pm s.d. ($n = 3$). * $P < 0.05$ versus Koshihikari (Student's *t*-test).



large and small vascular bundles (LVB and SVB, respectively; Fig. 7b–f). Because the majority of rice leaf tissue consists of mesophyll cells, we examined mesophyll cell number and size in cross-sections of flag leaves. Although mean mesophyll cell size did not differ between each parental cultivar and the corresponding NIL-GPS, the Takanari allele increased mesophyll cell number between the vascular bundles (Fig. 7g, h), and consequently enlarged the total mesophyll area between the vascular bundles in the cross-sections (Fig. 7i). The Takanari allele did not increase the distance between

vascular bundles and in some cases decreased it slightly (Fig. 7j). Taken together, these results suggest that increased mesophyll cell number produced thicker flag leaves and ultimately led to higher photosynthesis rate per unit leaf area in plants with the Takanari allele.

Selection of GPS in rice breeding history. Takanari is descended from high-yielding rice cultivars, including IR8, IR24, and the Korean high-yielding cultivar Tongil³⁷ (Fig. 1a). To examine

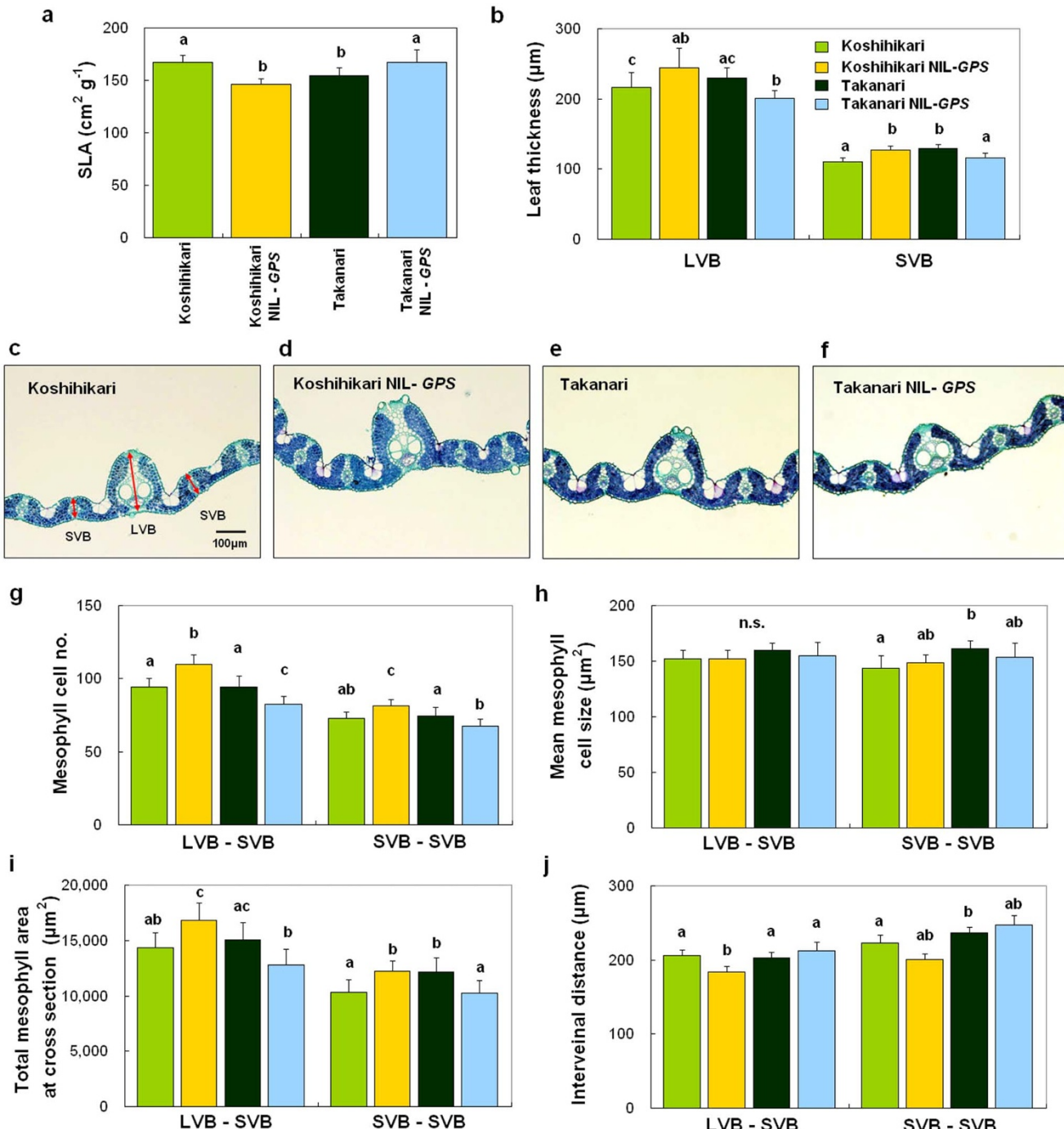


Figure 7 | Leaf anatomical characteristics controlled by GPS. (a, b) Comparison of specific leaf area (SLA) (a) and thickness (b) of flag leaves in Koshihikari, Koshihikari NIL-GPS, Takanari, and Takanari NIL-GPS. LVB, large vascular bundle, SVB, small vascular bundle. (c–f) Cross-sections of flag leaves stained with toluidine blue in Koshihikari (c), Koshihikari NIL-GPS (d), Takanari (e), and Takanari NIL-GPS (f). (g–j) Comparisons of mesophyll cell number (g), mean mesophyll cell size (h), total mesophyll area of cross-section (i), and interveinal distance (j) between LVB and SVB and between SVBs in the four genotypes. Each column represents mean \pm s.d. ($n = 9$). Different letters indicate significant difference at the 5% level (Tukey-Kramer HSD test).



whether the Takanari allele of *GPS* was selected in high-yield breeding programs, we analysed the nucleotide sequences of *NAL1* from 14 cultivars in the pedigree of Takanari for which seeds were available. The sequences could be classified into five haplotypes, and high-yielding cultivars such as IR8, IR24, and Tongil were categorized into the same haplotype as Takanari (Supplementary Table S2). Although there is no direct evidence that the Takanari allele originated from IR8, we discovered that IR8 inherited the allele from Peta and that Tongil inherited the allele from IR8 (Fig. 1a). These results suggest that rice breeders have repeatedly selected this favourable allele for photosynthesis in breeding programs for high yield.

Effects of *GPS* on productivity. To examine whether *GPS* affects rice productivity, we conducted yield trials with Koshihikari, Takanari, and the reciprocal NILs-*GPS*. In this experiment, Takanari and Takanari NIL-*GPS* were compared under high-N conditions, because higher yield can be achieved in Takanari and related materials under high N inputs. On the other hand, Koshihikari and Koshihikari NIL-*GPS* were compared under standard-N conditions because of their tendency to lodge. Takanari had higher grain yield than Takanari NIL-*GPS* owing to higher ripening percentage and 1000-grain weight (Table 1). These results indicate the importance of the Takanari allele of *GPS* for the performance of Takanari. However, grain yield was similar between Koshihikari and Koshihikari NIL-*GPS* (Table 1). The result suggests that other factors in addition to the Takanari allele of *GPS* are necessary to enhance grain yield in the Koshihikari genetic background.

Discussion

Until now, genetic factors underlying natural variation in photosynthesis rate have not been identified, because photosynthesis is rapidly affected by environmental changes and is hard to measure precisely for a large number of lines in a single experiment. We measured leaf photosynthesis only in the morning on clear days, because leaf photosynthesis did not reach its maximum levels on cloudy days or in the afternoon^{38,39}. The reciprocal materials also facilitated precise mapping of QTLs for photosynthesis rate, because the use of two populations enabled us to compare the positions of QTLs and the effects of QTL alleles between the two populations. By these methods, we identified *GPS*, a QTL that regulates photosynthesis rate in rice.

We revealed that *GPS* did not affect stomatal conductance (Supplementary Fig. S4a) but did change carboxylation efficiency by regulating Rubisco content under our experimental conditions (Fig. 2f, g, Fig 3b). Because Rubisco is a key enzyme in CO₂ fixation during photosynthesis, many research groups are attempting to improve Rubisco activity by using transgenic technology^{40–42}. Although *GPS* might not be involved in the activity of Rubisco, it is involved in controlling the amount of Rubisco (Fig. 2f, g). Therefore, our results show that manipulation of Rubisco content by using *GPS* is an effective strategy to enhance carboxylation efficiency and consequently photosynthesis rate.

High-resolution mapping and subsequent mutant and transgenic experiments revealed that *GPS* was identical to *NAL1*, which encodes a plant-specific protein involved in controlling lateral leaf growth³². Although the relationship between *NAL1* and photosynthesis was not tested at all in the previous study³², the discovery that *GPS* and *NAL1* are the same locus led us to hypothesize that the leaf morphological modifications produced by *NAL1* affect leaf photosynthesis properties. Our subsequent investigation of flag leaf anatomy revealed that *NAL1* (*GPS*) controlled not only lateral leaf growth, but also vertical leaf growth, namely leaf thickness, by modulating mesophyll cell divisions between vascular bundles (Fig. 7). Because leaf mesophyll cells are the major site of photosynthesis¹⁸ and make up the majority of rice leaf tissue (Fig. 7c–f), an increase in the number of mesophyll cells without size reduction or lateral extension can expand the vertical mesophyll tissue volume. Our results demonstrate the importance of *NAL1* (*GPS*) in the development of flag leaves, where it led to modulation of leaf N, Rubisco, and chlorophyll contents per unit leaf area and thereby contributed to carboxylation efficiency and leaf photosynthesis. Moreover, *NAL1* (*GPS*) also regulated leaf N, Rubisco, and chlorophyll contents per unit fresh or dry mass (Fig. 2e, g, i, Fig. 5d, i), which was reflected in photosynthesis rate per unit dry mass (Fig. 2c). Because these trait values expressed per unit fresh or dry mass reflect concentration, *NAL1* (*GPS*) may also regulate the amount of photosynthesis machinery per mesophyll cell, which may also contribute to carboxylation efficiency and leaf photosynthesis.

The importance of thicker leaves in relation to photosynthesis has been evident for a long time from observations that sun leaves are thicker, have more photosynthesis machinery per cell, and show higher photosynthesis rate than shade leaves^{34,43}. However, little is known about genes controlling leaf thickness and photosynthesis rate, although these two traits show a close relationship in diverse plant species and show varietal differences^{35,44}. In this study, we revealed that *NAL1* had pleiotropic effects on leaf anatomy and photosynthesis. Interestingly, a similar function has been reported for the *Arabidopsis ERECTA* gene⁴⁵, which encodes a putative leucine-rich-repeat receptor protein kinase⁴⁶. The functional allele of *ERECTA* led to a greater number of mesophyll cells, tighter packing of mesophyll cells, and higher carboxylation efficiency than loss-of-function alleles⁴⁵. However, unlike *NAL1*, *ERECTA* was also associated with epidermal morphology. The functional allele of *ERECTA* reduced stomatal density and thereby lowered stomatal conductance relative to loss-of-function alleles; for this reason, *ERECTA* is regarded as a transpiration efficiency gene. Recently, rice mutants generated by artificial mutagens were screened for mesophyll cell architecture with the goal of improving photosynthetic capacity⁴⁷. Several mutant lines showed favourable alterations such as increased mesophyll cell size. However, none of them had an enhanced photosynthesis rate relative to wild-type plants⁴⁸. Because artificial mutations often cause detrimental side effects, these effects may have cancelled out the effects of the favourable mesophyll alterations necessary for improved photosynthesis rate. In this context, natural

Table 1 | Yield and yield components in Koshihikari, Koshihikari NIL-*GPS*, Takanari, and Takanari NIL-*GPS*

Cultivar or NIL	Yield (g m ⁻²)	Spikelets (no. m ⁻²)	Ripening (%)	1000-grain wt. (g)
Koshihikari	560	29,968	84.2	21.7
Koshihikari NIL- <i>GPS</i> (n = 3)	559 n.s.	28,029 n.s.	86.1 n.s.	22.8 **
Takanari	1,051	59,217	83.1	21.0
Takanari NIL- <i>GPS</i> (n = 5)	1,002 *	60,797 n.s.	78.4 *	20.5 **

N fertilization was 6 g N m⁻² for Koshihikari and its NIL-*GPS* and 18 g N m⁻² for Takanari and its NIL-*GPS*.

**P < 0.01;

*P < 0.05; n.s., not significant (Student's t-test).

Comparisons were made between each cultivar and the corresponding NIL-*GPS*.



variations of *NAL1* (*GPS*) and *ERECTA* are valuable for obtaining enhanced photosynthesis capacity through leaf anatomical modifications.

With regard to detrimental side effects, T65-*nall* and RNAi-*NAL1* plants showed severe dwarf plant stature not seen in Koshihikari NIL-*GPS* (Fig. 2a, Fig. 5a, f), although all three of these materials displayed an increase in photosynthesis rate. The differences in phenotype might be attributable to the level of *NAL1* function. The 30-bp deletion in the fourth exon in T65-*nall* and the reduction of *NAL1* expression induced by RNAi seem to have caused severe loss-of-function of *NAL1*. On the other hand, the reduced *NAL1* protein level in Takanari compared with Koshihikari and the presence of three amino acid substitutions between the two cultivars suggest partial loss-of-function of the *NAL1* encoded by the Takanari allele. Other cases have been reported in which a moderate level of gene function produces a preferable plant phenotype⁴⁹. For example, *APO1*, which controls panicle structure, increased spikelet number per panicle with no decline in panicle number when expressed to a level twice that of the wild type, but caused a remarkable decline in panicle number when overexpressed to levels much higher than that of the wild type^{50,51}. The partial loss-of-function allele of *GN1a* also increased spikelet number per panicle, with only a slight decrease in panicle number, compared with the gain-of-function allele⁵. On the basis of these results, we suggest that a weak *NAL1* allele such as the Takanari allele of *GPS* increases the photosynthesis rate without detrimental side effects and is suitable for breeding. This is supported by the fact that the Takanari allele appears to have been repeatedly selected in high-yield breeding programs (Fig. 1a). While it is well known that the semi-dwarf gene *sd1* was selected from Dee-geo-woo-gen when IR8 was developed⁵², IR8 also contains the Takanari allele of *GPS* that was inherited from Peta (Fig. 1a). Likewise, the *GPS* allele from IR8 is present in Tongil, the first high-yielding cultivar in Korea (Fig. 1a). After several more generations of breeding and selection, Takanari inherited this allele, although we could not determine the original cultivar that contributed the allele to Takanari because it is found in several ancestors of Takanari. These facts provide strong evidence that breeders regarded the phenotype conferred by the Takanari allele of *GPS* as an important factor when developing high-yielding cultivars. The contribution of Dee-geo-woo-gen as the source of *sd1* has frequently been highlighted in discussions of the “Green Revolution” in rice. Our results reveal the importance of another gene that the traditional cultivar Peta provided to IR8 and subsequent high-yielding cultivars. But how did breeders select an allele for higher photosynthesis without directly observing photosynthesis? One possibility is that breeders might have used leaf colour as a selection criterion, because the Takanari allele of *GPS* produces dark green leaves (Fig. 2a, Fig. 6a). Thick, dark green leaves were also targeted in new-plant-type (NPT) breeding in the 1990s⁵³. Because high photosynthesis rates and dark green leaves are common to Takanari, IR8, and Tongil²⁶, the Takanari allele of *GPS* is likely to have been selected through leaf colour.

The ultimate goal of our studies of *GPS* is to increase rice yield potential. Thus, we examined grain yield of Koshihikari, Takanari, and the reciprocal NILs-*GPS*, and discovered that the Takanari allele of *GPS* was indispensable for Takanari to achieve its normal yield level (Table 1). On the other hand, the Takanari allele did not increase grain yield in Koshihikari (Table 1). When yield components were compared between Koshihikari and Koshihikari NIL-*GPS*, we found no significant difference in spikelet number per m², but found a slight increase in ripening percentage and a significant increase in 1000-grain weight for Koshihikari NIL-*GPS* (Table 1). The comparison indicates that combination of *GPS* with sink size QTLs such as *GN1a* and *APO1* may be necessary to increase grain yield in the Koshihikari background. An alternative is that *GPS* may require high N inputs to have maximum effect on yield.

We found that *GPS*, a newly identified QTL regulating photosynthesis rate, is identical to *NAL1*, a gene previously identified for its effects on plant morphology. To our knowledge, *NAL1* is the first gene shown to account for natural variation in rice photosynthesis rate, although its molecular function is still unknown. Nevertheless, this finding opens up possibilities for further identification of other photosynthesis-related QTLs and further understanding of the genetic mechanisms underlying natural variation in photosynthesis rate. Combining photosynthesis QTLs with sink size QTLs will enhance future high-yield breeding and provide a new and efficient strategy for increased rice productivity.

Methods

Plant growth conditions. Field experiments were conducted in a paddy field at the NARO Institute of Crop Science, Ibaraki, Japan, and at the University Farm, Tokyo University of Agriculture and Technology, Tokyo, Japan. Seeds were sown in nursery boxes, and 21-day-old seedlings were transplanted at a density of one seedling per hill, at a spacing of 15 cm between hills and 30 cm between rows. For the QTL mapping experiments and for yield trials in standard-N plots, basal fertilizer was applied at 60 kg N, 52 kg P, and 75 kg K ha⁻¹. For yield trials in high-N plots, N was applied at 180 kg ha⁻¹ (120 kg as basal fertilizer and 60 kg as topdressing at the panicle initiation stage), with 70 kg P and 100 kg K ha⁻¹ as basal fertilizer. Experimental plots for yield trials were arranged in a randomized complete block design with three or five replications.

Plant materials and QTL mapping. For QTL analysis of leaf photosynthesis, reciprocal BILs (BC_1F_6) were developed between a high-yielding *indica* rice cultivar, Takanari, and a leading *japonica* cultivar, Koshihikari, both grown in Japan. The reciprocal BILs consisted of 87 lines each in the Koshihikari and Takanari genetic backgrounds, but some lines were excluded because of hybrid weakness or extremely late heading; thus, 82 and 86 lines, respectively, were used for QTL analysis. The genome-wide genotype of each line was determined by using 140 PCR-based DNA markers, and linkage maps were constructed with MAPMAKER/EXP 3.0 software⁵⁴. The chromosomal positions and effects of putative QTLs were determined by composite interval mapping with QTL Cartographer 2.0 software⁵⁵. The threshold of QTL detection was based on 1000 permutation tests at the 5% level of significance. The reciprocal NILs-*GPS* were developed through four generations of backcrossing and marker-assisted selection. For map-based cloning, we used F_2 progeny derived from crosses of each NIL-*GPS* to the corresponding recurrent parent cultivar. Consequently, 26 and 24 plants with recombination near the QTL were identified from 8308 and 2784 F_2 plants in the Koshihikari and Takanari genetic backgrounds, respectively. The primer sets for the InDel markers used in map-based cloning are listed in Supplementary Table S3.

Leaf photosynthesis measurement. Leaf photosynthesis was measured in flag leaves at the full heading stage with a portable photosynthesis system (LI-6400; Li-Cor). Measurement was conducted on clear days between 0900 and 1300 h under a constant saturated light level of 2000 $\mu\text{mol m}^{-2} \text{s}^{-1}$ provided by red/blue light-emitting diodes. The leaf chamber temperature was maintained at 30°C, the reference CO₂ concentration was 390 $\mu\text{mol mol}^{-1}$, and the mean leaf-to-air vapour pressure difference was 1.1 kPa. Gas-exchange parameters were recorded once the topmost expanded leaf was enclosed in the chamber and the photosynthesis rate reached steady state. Leaf photosynthesis was also measured at different light levels between 0 and 2000 $\mu\text{mol m}^{-2} \text{s}^{-1}$ and different reference CO₂ concentrations between 0 and 1500 $\mu\text{mol mol}^{-1}$. To fit the biochemical Farquhar model of C₃ photosynthesis to CO₂ response data²⁹, we used the Rubisco kinetic parameters determined by the temperature response functions⁵⁶. Leaf N, Rubisco, and chlorophyll contents were investigated using the same flag leaves for which leaf photosynthesis was measured in the field. Leaf N was quantified with an NC analyser (Sumigraph NCH-22F; Sumik Chemical Analysis Service). Rubisco was quantified by the single radial immunodiffusion method with rabbit polyclonal antibodies raised against purified Rubisco from rice²⁸. Chlorophyll content was determined by extraction with N,N'-dimethylformamide (DMF)⁵⁷.

Observation of the cross-section of flag leaves. After leaf photosynthesis was measured, central sections of flag leaf blades were sampled, fixed in 4% paraformaldehyde/0.25% glutaraldehyde fixative solution, and embedded in paraffin wax. Transverse sections of leaves 7 μm thick were cut on a rotary microtome (HM335E; Microm) and stained with 0.05% toluidine blue. Leaf mesophyll anatomy at the second large vascular bundles from the midrib was observed under a fluorescence microscope (BX51N-34-FL; Olympus) at $\times 200$ magnification and analysed with digital image processing software (Win-ROOF v. 6.1; Mitani). To measure the distance between vascular bundles, stomatal density, and stomatal length, we observed the abaxial epidermis of fixed flag leaves under a scanning electron microscope (SEM) (VE-9800; Keyence) and analysed the measurements with Win-ROOF.

Transformation of rice with RNAi construct. To produce a construct for knockdown of *NAL1*, we amplified a gene-specific DNA fragment of 308 bp



including the fifth exon and 3' UTR of *NAL1* by PCR using specific primers (Supplementary Table S3). The fragments were cloned in head-to-head orientation into the RNA interference vector pZH2Bik (a generous gift from M. Kuroda)⁵⁸. This plasmid was introduced into callus derived from Koshihikari by a high-efficiency *Agrobacterium*-mediated transformation system for rice callus⁵⁹.

RNA isolation and expression and transcript analysis. Total RNA was extracted from flag leaf tissues at each developmental stage by using an RNeasy Mini Kit (Qiagen). First-strand cDNA was synthesized by using SuperScript III reverse transcriptase (Invitrogen). Quantitative real-time PCR (qRT-PCR) was performed by using SYBR Green Realtime PCR Master Mix (Toyobo) and specific primers (Supplementary Table S3) on an ABI7300 system (Applied Biosystems). The results were confirmed by analysing four biological replicates, with three technical repeats for each biological replicate. The *UBQ2* gene from rice was used as an internal standard (Supplementary Table S3). For transcript analysis, cDNA was amplified by specific primers of 5'-UTR and 3'-UTR (Supplementary Table S3). The PCR products were cloned by using Zero Blunt TOPO PCR Cloning Kit (Invitrogen) and sequenced with a BigDye Terminator v. 3.1 Cycle Sequencing Kit (Applied Biosystems) on an automated fluorescent laser sequencer (3130xl; Applied Biosystems).

Western blot analysis. Antiserum to *NAL1* was generated by injection of rabbits with the synthetic oligopeptide SPVRDDQDAPRSITN, corresponding to the C-terminal region of *NAL1*. Total protein was extracted from flag leaf tissues at the full heading stage and quantified by the Bradford method⁶⁰. The protein (14 µg) was subjected to SDS-PAGE in 10% polyacrylamide gel for separation and electro-transferred onto polyvinylidene difluoride (PVDF) membranes (Bio-Rad Laboratories), which were then incubated with rabbit antiserum to *NAL1*. The *NAL1* oligopeptide antibodies were used at a 1:1000 dilution. Immunodetection was performed with an ECL Plus western blotting kit (GE Healthcare) on a luminescent image analyser (LAS-3000; Fujifilm).

Sequence analysis. For comparison of *NAL1* sequences among cultivars in the pedigree of Takanari, the *NAL1* genomic regions were amplified by PCR with seven primer sets (Supplementary Table S3). The PCR products were sequenced with a BigDye Terminator v. 3.1 Cycle Sequencing Kit (Applied Biosystems) on an automated fluorescent laser sequencer (3130xl; Applied Biosystems).

Statistical analysis. All statistical analyses were done with JMP v. 8.0 software (SAS Institute).

1. Hargrove, T. R. & Cabanilla, V. L. The impact of semidwarf varieties on Asian rice breeding programs. *Bioscience* **29**, 731–735 (1979).
2. Khush, G. S. Green revolution: the way forward. *Nat. Rev. Genet.* **2**, 815–822 (2001).
3. Tester, M. & Langridge, P. Breeding technologies to increase crop production in a changing world. *Science* **327**, 818–822 (2010).
4. Foley, J. A. *et al.* Solutions for a cultivated planet. *Nature* **478**, 337–342 (2011).
5. Ashikari, M. *et al.* Cytokinin oxidase regulates rice grain production. *Science* **309**, 741–745 (2005).
6. Terao, T., Nagata, K., Morino, K. & Hirose, T. A gene controlling the number of primary rachis branches also controls the vascular bundle formation and hence is responsible to increase the harvest index and grain yield in rice. *Theor. Appl. Genet.* **120**, 875–893 (2010).
7. Miura, K. *et al.* *OsSPL14* promotes panicle branching and higher grain productivity in rice. *Nat. Genet.* **42**, 545–549 (2010).
8. Song, X. J., Huang, W., Shi, M., Zhu, M. Z. & Lin, H. X. A QTL for rice grain width and weight encodes a previously unknown RING-type E3 ubiquitin ligase. *Nat. Genet.* **39**, 623–630 (2007).
9. Fan, C. *et al.* GS3, a major QTL for grain length and weight and minor QTL for grain width and thickness in rice, encodes a putative transmembrane protein. *Theor. Appl. Genet.* **112**, 1164–1171 (2006).
10. Shomura, A. *et al.* Deletion in a gene associated with grain size increased yields during rice domestication. *Nat. Genet.* **40**, 1023–1028 (2008).
11. Li, Y. *et al.* Natural variation in GS5 plays an important role in regulating grain size and yield in rice. *Nat. Genet.* **43**, 1266–1269 (2011).
12. Ohsumi, A. *et al.* Evaluation of yield performance in rice near-isogenic lines with increased spikelet number. *Field Crops Res.* **120**, 68–75 (2011).
13. Yoshida, H., Horie, T. & Shiraiwa, T. A model for explaining genotypic and environmental variation in vegetative biomass growth in rice based on observed LAI and leaf nitrogen content. *Field Crops Res.* **108**, 222–230 (2008).
14. Yoshida, H. & Horie, T. A process model for explaining genotypic and environmental variation in growth and yield of rice based on measured plant N accumulation. *Field Crops Res.* **113**, 227–237 (2009).
15. Sasaki, H. & Ishii, R. Cultivar differences in leaf photosynthesis of rice bred in Japan. *Photosynthesis Res.* **32**, 139–146 (1992).
16. Hubbard, S., Peng, S., Horton, P., Chen, Y. & Murchie, E. H. Trends in leaf photosynthesis in historical rice varieties developed in the Philippines since 1966. *J. Exp. Bot.* **58**, 3429–3438 (2007).
17. Farquhar, G. D. & Sharkey, T. D. Stomatal conductance and photosynthesis. *Annu. Rev. Plant Physiol.* **33**, 317–345 (1982).
18. Lambers, H., Chapin III, F. S. & Pons, T. L. *Plant Physiological Ecology*. (Springer Verlag, 1998).
19. Evans, J. R. Photosynthesis and nitrogen relationships in leaves of C₃ plants. *Oecologia* **78**, 9–19 (1989).
20. Makino, A. Rubisco and nitrogen relationships in rice: Leaf photosynthesis and plant growth. *Soil Sci. Plant Nutr.* **49**, 319–327 (2003).
21. Kanemura, T., Homma, K., Ohsumi, A., Shiraiwa, T. & Horie, T. Evaluation of genotypic variation in leaf photosynthetic rate and its associated factors by using rice diversity research set of germplasm. *Photosynthesis Res.* **94**, 23–30 (2007).
22. Ohsumi, A. *et al.* A model explaining genotypic and ontogenetic variation of leaf photosynthetic rate in rice (*Oryza sativa*) based on leaf nitrogen content and stomatal conductance. *Ann. Bot.* **99**, 265–273 (2007).
23. Xing, Y. Z. & Zhang, Q. F. Genetic and molecular bases of rice yield. *Annu. Rev. Plant Biol.* **61**, 421–442 (2010).
24. Flood, P. J., Harbinson, J. & Aarts, M. G. Natural genetic variation in plant photosynthesis. *Trends Plant Sci.* **16**, 327–335 (2011).
25. Tayalaran, R. D., Adachi, S., Ookawa, T., Usuda, H. & Hirasawa, T. Hydraulic conductance as well as nitrogen accumulation plays a role in the higher rate of leaf photosynthesis of the most productive variety of rice in Japan. *J. Exp. Bot.* **62**, 4067–4077.
26. Takai, T. *et al.* Comparative mapping suggests repeated selection of the same quantitative trait locus for high leaf photosynthesis rate in rice high-yield breeding programs. *Crop Sci.* **52**, 2649–2658 (2012).
27. Takai, T., Kondo, M., Yano, M. & Yamamoto, T. A quantitative trait locus for chlorophyll content and its association with leaf photosynthesis in rice. *Rice* **3**, 172–180 (2010).
28. Adachi, S. *et al.* Identification and characterization of genomic regions on chromosomes 4 and 8 that control the rate of photosynthesis in rice leaves. *J. Exp. Bot.* **62**, 1927–1938 (2011).
29. Farquhar, G. D., von Caemmerer, S. & Berry, J. A. A biochemical model of photosynthetic CO₂ assimilation in leaves of C₃ species. *Planta* **149**, 78–90 (1980).
30. Rice Annotation Project. The Rice Annotation Project Database (RAP-DB): 2008 update. *Nucleic Acids Res.* **36**, D1028–1033 (2008).
31. Yamamoto, T. *et al.* Fine definition of the pedigree haplotypes of closely related rice cultivars by means of genome-wide discovery of single-nucleotide polymorphisms. *BMC Genomics* **11**, 267 (2010).
32. Qi, J. *et al.* Mutation of the rice *Narrow leaf1* gene, which encodes a novel protein, affects vein patterning and polar auxin transport. *Plant Physiol.* **147**, 1947–1959 (2008).
33. Chen, M. *et al.* Fine mapping of a major QTL for flag leaf width in rice, *qFLW4*, which might be caused by alternative splicing of *NAL1*. *Plant Cell Rep.* **31**, 863–872 (2011).
34. Boardman, N. K. Comparative photosynthesis of sun and shade plants. *Annu. Rev. Plant Physiol.* **28**, 355–377 (1977).
35. Niinemets, U. Components of leaf dry mass per area—thickness and density—alter leaf photosynthetic capacity in reverse directions in woody plants. *New Phytol.* **144**, 35–47 (1999).
36. Vile, D. *et al.* Specific leaf area and dry matter content estimate thickness in laminar leaves. *Ann. Bot.* **96**, 1129–1136 (2005).
37. Chung, G. S. & Heu, M. H. *Innovative Approaches to Rice Breeding*, 135–152 (IRRI, 1980).
38. Ishihara, K. & Saito, K. Diurnal courses of photosynthesis, transpiration, and diffusive conductance in the single-leaf of the rice plants grown in the paddy field under submerged condition. *Japan. J. Crop Sci.* **56**, 8–17 (1987).
39. Takai, T., Yano, M. & Yamamoto, T. Canopy temperature on clear and cloudy days can be used to estimate varietal differences in stomatal conductance in rice. *Field Crops Res.* **115**, 165–170 (2010).
40. Ishikawa, C., Hatanaka, T., Misoo, S., Miyake, C. & Fukayama, H. Functional incorporation of sorghum small subunit increases the catalytic turnover rate of Rubisco in transgenic rice. *Plant Physiol.* **156**, 1603–1611 (2011).
41. Whitney, S. M. *et al.* Isoleucine 309 acts as a C₄ catalytic switch that increases ribulose-1,5-bisphosphate carboxylase/oxygenase (rubisco) carboxylation rate in Flaveria. *Proc. Natl. Acad. Sci. USA* **108**, 14688–14693 (2011).
42. Yamori, W., Masumoto, C., Fukayama, H. & Makino, A. Rubisco activase is a key regulator of non-steady-state photosynthesis at any leaf temperature and, to a lesser extent, of steady-state photosynthesis at high temperature. *Plant J.* **71**, 871–880 (2012).
43. Terashima, I., Hanba, Y., Tazoe, T., Vyas, P. & Yano, S. Irradiance and phenotype: comparative eco-development of sun and shade leaves in relation to photosynthetic CO₂ diffusion. *J. Exp. Bot.* **57**, 343–354 (2006).
44. Pearce, R. B., Carlson, G. E., Barnes, D. K., Hart, R. H. & Hanson, C. H. Specific leaf weight and photosynthesis in Alfalfa. *Crop Sci.* **9**, 423–426 (1969).
45. Masle, J., Gilmore, S. R. & Farquhar, G. D. The *ERECTA* gene regulates plant transpiration efficiency in *Arabidopsis*. *Nature* **436**, 866–870 (2005).
46. Torii, K. U. *et al.* The *Arabidopsis ERECTA* gene encodes a putative receptor protein kinase with extracellular leucine-rich repeats. *Plant Cell* **8**, 735–746 (1996).
47. Smillie, I. R., Pyke, K. A. & Murchie, E. H. Variation in vein density and mesophyll cell architecture in a rice deletion mutant population. *J. Exp. Bot.* **63**, 4563–4570 (2012).



48. Smillie, I. R. A. *Analysis of leaf morphology and photosynthesis in deletion mutants of rice (*Oryza sativa L.*)* Ph.D. thesis available at <http://etheses.nottingham.ac.uk/2569/> (University of Nottingham, 2012).
49. Takeda, S. & Matsuoka, M. Genetic approaches to crop improvement: responding to environmental and population changes. *Nat. Rev. Genet.* **9**, 444–457 (2008).
50. Ikeda-Kawakatsu, K. *et al.* Expression level of *ABERRANT PANICLE ORGANIZATION1* determines rice inflorescence form through control of cell proliferation in the meristem. *Plant Physiol.* **150**, 736–747 (2009).
51. Ookawa, T. *et al.* New approach for rice improvement using a pleiotropic QTL gene for lodging resistance and yield. *Nat. Commun.* **1**, 132 (2010).
52. Sasaki, A. *et al.* A mutant gibberellin-synthesis gene in rice. *Nature* **416**, 701–702 (2002).
53. Peng, S., Cassman, K. G., Virmani, S. S., Sheehy, J. & Khush, G. S. Yield potential trends of tropical rice since the release of IR8 and the challenge of increasing rice yield potential. *Crop Sci.* **39**, 1552–1559 (1999).
54. Lander, E. S. *et al.* MAPMAKER: an interactive computer package for constructing primary genetic linkage maps of experimental and natural populations. *Genomics* **1**, 174–181 (1987).
55. QTL Cartographer. Version 1.16. *A Reference Manual and Tutorial for QTL Mapping* (North Carolina State University, 2002).
56. Bernacchi, C. J., Singsaas, E. L., Pimentel, C., Portis, J. R. & Long, S. P. Improved temperature response functions for models of Rubisco-limited photosynthesis. *Plant Cell Environ.* **24**, 253–259 (2001).
57. Porra, R. J., Thompson, W. A. & Kriedemann, P. E. Determination of accurate extinction coefficients and simultaneous equations for assaying chlorophylls *a* and *b* extracted with four different solvents: verification of the concentration of chlorophyll standards by atomic absorption spectroscopy. *Biochim. Biophys. Acta* **975**, 384–394 (1989).
58. Kuroda, M., Kimizu, M. & Mikami, C. A simple set of plasmids for the production of transgenic plants. *Biosci. Biotechnol. Biochem.* **74**, 2348–2351 (2010).
59. Ozawa, K. Establishment of a high efficiency *Agrobacterium*-mediated transformation system of rice (*Oryza sativa L.*). *Plant Sci.* **176**, 522–527 (2009).
60. Bradford, M. M. A rapid and sensitive method for the quantitation of microgram quantities of protein utilizing the principle of protein-dye binding. *Anal. Biochem.* **72**, 248–254 (1976).

Acknowledgments

The *nali* mutant line was kindly provided by the National Institute of Genetics (Oryzabase, available at <http://www.shigen.nig.ac.jp/rice/oryzabaseV4/>). Seeds of the reciprocal BILs between Koshihikari and Takanari can be obtained from the Rice Genome Resource Center (<http://www.rgrc.dna.affrc.go.jp/index.html>). This work was supported by a grant from the Ministry of Agriculture, Forestry and Fisheries of Japan (Genomics for Agricultural Innovation, QTL002 and NVR-0001).

Author contributions

T.T. and T.Y. designed the experiments and wrote the manuscript. T.T., T.I., and T.Y. developed the reciprocal BILs. T.T., S.A., T.H., and T.Y. performed phenotyping for cloning GPS. T.T., T.A., I.K., S.I., A.S., and T.Y. performed genotyping for cloning GPS. J.W. and T.M. performed BAC clone analysis. T.T. and F.T.-S. performed sequencing analysis. T.T., U.Y., S.H., Y.T., and T.Y. performed molecular analysis. T.T., Y.S.-A., N.I., S.Y., and M.K. performed yield trials. K.S., K.K., T.O., T.H., M.Y., and M.K. provided advice on the experiments.

Additional information

Supplementary information accompanies this paper at <http://www.nature.com/scientificreports/>

Competing financial interests: The authors declare no competing financial interests.

How to cite this article: Takai, T. *et al.* A natural variant of *NAL1*, selected in high-yield rice breeding programs, pleiotropically increases photosynthesis rate. *Sci. Rep.* **3**, 2149; DOI:10.1038/srep02149 (2013).

This work is licensed under a Creative Commons Attribution-NonCommercial-ShareAlike 3.0 Unported license. To view a copy of this license, visit <http://creativecommons.org/licenses/by-nc-sa/3.0>